Dams and Reservoirs under Changing Challenges – Schleiss & Boes (Eds)
© 2011 Taylor & Francis Group, London, ISBN 978-0-415-68267-1

Effects of vertical earthquake motions on deformation of Newmark sliding analysis

N. Matsumoto, T. Sasaki & K. Shimamoto
Japan Dam Engineering Center, Tokyo, Japan

Y. Sugiura & H.Q. Zhao
CREARIA, Tokyo, Japan

ABSTRACT: Newmark procedure is one of the methods to predict earthquake-induced deformations of embankment dams. It assumes that the sliding mass is rigid and the mass begins to move when the safety factor of the sliding mass becomes less than 1.0 and cease to move when the velocity of the sliding mass becomes equal to the rest of the embankment. Most of the Newmark procedures are based on the equilibrium equation of one-dimensional horizontal motion ignoring the vertical component. According to recent strong motion monitoring, large vertical accelerations were recorded. Hence the inertia force of vertical component is introduced in the paper. By using sinusoidal and recorded earthquake acceleration records, the earthquake-induced deformations were computed and the effects of vertical motion on permanent deformation of embankment dams are described.

1 INTRODUCTION

Newmark proposed the deformation based procedure for the assessment of the seismic stability of embankment dams (Newmark, 1965). In his procedure, an earth mass sliding over a shear surface was modeled as a rigid block sliding over a plane assuming the stress-strain relationship to be rigid-plastic. In reality, embankment materials show volumetric strain and softening property to cyclic loading, so the Newmark procedure is considered as a tool for the first approximation. But in this method input parameters are identical to those of the slope stability analysis and it provides relatively reasonable results which are easily interpreted with clear assumption.

Modifications have been proposed to Newmark's sliding block procedure since its first formulation. In most cases, however, only horizontal accelerations were included with a few exceptions. Yan proposed a rigid block on an inclined plane slip surface and also a rigid block on a circular arc slip surface and in both cases vertical motions are included (Yan, 1991). Later, Yan et al. computed the effects of vertical motion on permanent displacements for two slopes and two earthquake records (Yan et al., 1996). Their results indicate that the introduction of the vertical component can both increase (11%) and decrease (–4%) the calculated displacements. Tateyama et al. introduced the idea of the rotating block (Tateyama et al., 1998) as shown in Figure 1. They gave the equation of motion for the rotating block considering horizontal earthquake inertia force by Equation 1.

$$-J\ddot{\theta} + M_{DW} + M_{DKh} - M_{RW} - M_{RKh} = 0 \tag{1}$$

where θ = angle of rotation; J = Inertia moment; M_{DW} = Driving moment due to gravity; M_{DKh} = Driving moment due to horizontal earthquake inertia force; M_{RW} = Resisting moment due to gravity; M_{RKh} = Resisting moment due to horizontal earthquake inertia force.

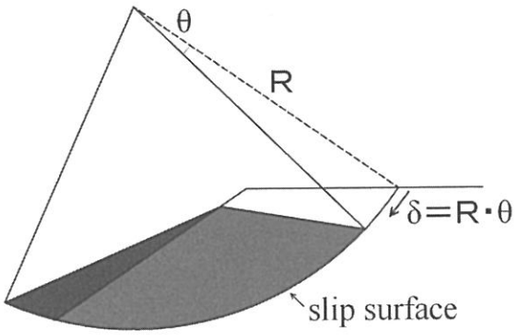

Figure 1. Rotating block.

If we take the vertical earthquake acceleration into consideration, Equation 1 is modified as follows:

$$-J\ddot{\theta}+M_{DW}+M_{DKh}+M_{DKv}-M_{RW}-M_{RKh}-M_{RKv}=0 \tag{2}$$

where M_{DKv} = Driving moment due to vertical earthquake inertia force; M_{RKv} = Resisting moment due to vertical earthquake inertia force.

The driving moments M_{DKh} and M_{DKv} can be computed from the acceleration distribution of the sliding block directly, or by using the average absolute acceleration k_h and k_v (Eq. 3). Comparing the driving moment from the average acceleration and the inertia force of each element, the difference was recognized as insignificant. Therefore, the average acceleration is used for obtaining the driving moment, hereafter.

$$k_h=\frac{\sum\rho_i\alpha_{hi}}{\sum\rho_i}\quad k_v=\frac{\sum\rho_i\alpha_{vi}}{\sum\rho_i} \tag{3}$$

where k_h = average horizontal acceleration in g; k_v = average vertical acceleration in g; ρ_i = mass of element i; α_{hi} = absolute acceleration of horizontal component of element i in g; α_{vi} = absolute acceleration of vertical component of element i in g.

The safety factor, F_s, during shaking is given by

$$Fs=\frac{M_{RW}+M_{RKh}+M_{RKv}}{M_{DW}+M_{DKh}+M_{DKv}}=\frac{(1+k_v)M_{RW}-k_hM_{Rh1}}{(1+k_v)M_{DW}+k_hM_{Dh1}} \tag{4}$$

where M_{Rh1} = Resisting moment when average horizontal acceleration is 1.0 g; M_{Dh1} = Driving moment when average horizontal acceleration is 1.0 g.

Resisting moment M_{Rh1}, M_{Rv1} can be obtained from the resisting force using normal stresses on the slip surface of the finite element or from ordinary method of slice of the block. Here, the latter procedure is adopted.

In Figure 2, when F_s becomes 1.0, the rotation of the block begins at $t = t_b$ and continues until the driving moment falls below the resisting moment and ends when the velocity falls to zero at $t = t_e$. The angular acceleration can be calculated by Equation 5.

$$\ddot{\theta}=\frac{(1+k_v)M_{DW}+k_hM_{Dh1}-(1+k_v)M_{RW}-k_hM_{Rh1}}{J} \tag{5}$$

The displacement or angular rotation of the block will be obtained by integrating the angular acceleration twice.

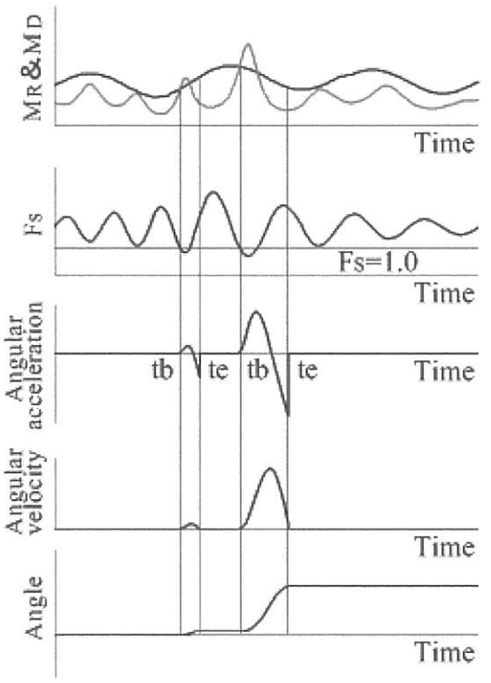

Figure 2. Stick-slip rotation of block mass.

2 ANALYTICAL MODEL AND MATERIAL PROPERTIES

Figure 3 is the finite element mesh used for the two-dimensional dynamic analyses to assess the earthquake-induced deformations. In this figure, 10 circular sliding blocks on the downstream side are shown. The dynamic material properties for each zone are shown in Table 1. Figure 4 shows the normalized modulus reduction ratio of filter and rockfill materials. Poisson's ratio is derived from Equation 6.

Core	$\nu = 0.450–0.006Z^{0.60}$	
Filter and rockfill	$\nu = 0.375–0.006Z^{0.58}$ (above the seepage surface)	(6)
	$\nu = 0.490–0.001Z^{0.95}$ (beneath the seepage surface)	

Where, Z is the depth from top surface of the dam body (m).

The strength for each zone used to calculate the sliding safety factor and sliding deformation are shown in Table 1. The shear strength of rockfill is assumed according to the curved failure envelope formula of $\tau_f = A(\sigma_n)^b$ and the shear strength of the core is expressed as cohesion concept c' and friction angle φ'.

3 YIELD ACCELERATION

The combination of the horizontal yield acceleration and vertical yield acceleration when F_s equals 1.0 computed from Equation 4 is shown in Figure 5. It suggests that the deeper the sliding surface is, the smaller the yield acceleration is. This is because of the curved shear strength envelop of the materials which means the internal friction angle decreases with the increase of the confining pressure. The vertical acceleration has greater effects on shallow sliding blocks than on deep ones. This is because the upward seismic inertia force reduces the resisting moment and the friction angle decreases more in the low confining pressure range of the curved failure envelope.

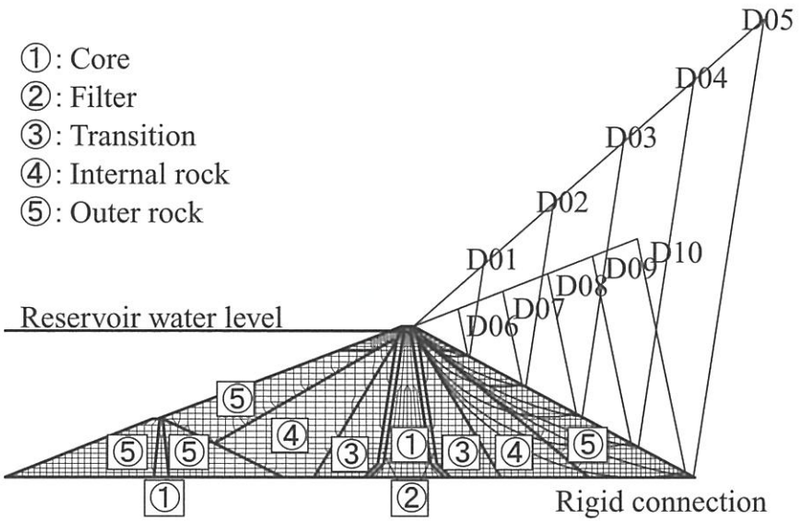

Figure 3. Finite element mesh with material zones and assumed sliding blocks with centres D_{01}–D_{10}.

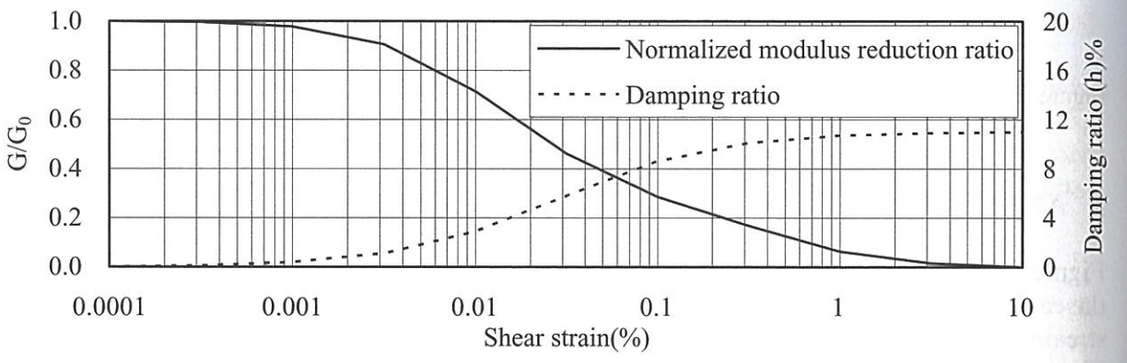

Figure 4. Normalized modulus reduction ratio and damping ratio used for analysis.

Table 1. Material properties for dynamic analysis and strength parameters used to calculate the sliding safety factor and earthquake-induced settlements.

Zone	Total unit weight (kN/m^3)	Shear modulus G_0 in MPa Vs in m/s Z in meter	Shear strength in kN/m^2			
			c'(kN/m^2)	φ'(°)	A	b
Core	22.5	$G_0 = 1.3 \times (\gamma_t \times Vs^2/9800)$ $Vs = 6.4Z + 314$	12.5	36.5	–	–
Filter	21.8		–	–	3.075	0.817
Transition	21.1	$G_0 = 1.3 \times (\gamma_t \times Vs^2/9800)$	–	–	3.482	0.805
Internal rock	21.2	$Vs = 5.1Z + 342$	–	–	4.039	0.777
Outer rock	20.8		–	–	3.769	0.792

4 EFFECTS OF INPUT VERTICAL MOTION

The response was compared for the case of horizontal motion input only and the case for both of horizontal and vertical motion input. Figure 6 shows the maximum acceleration distribution in the center of the dam with and without vertical motion input using acceleration record of Hitokura Dam in Table 2. The vertical input motion has

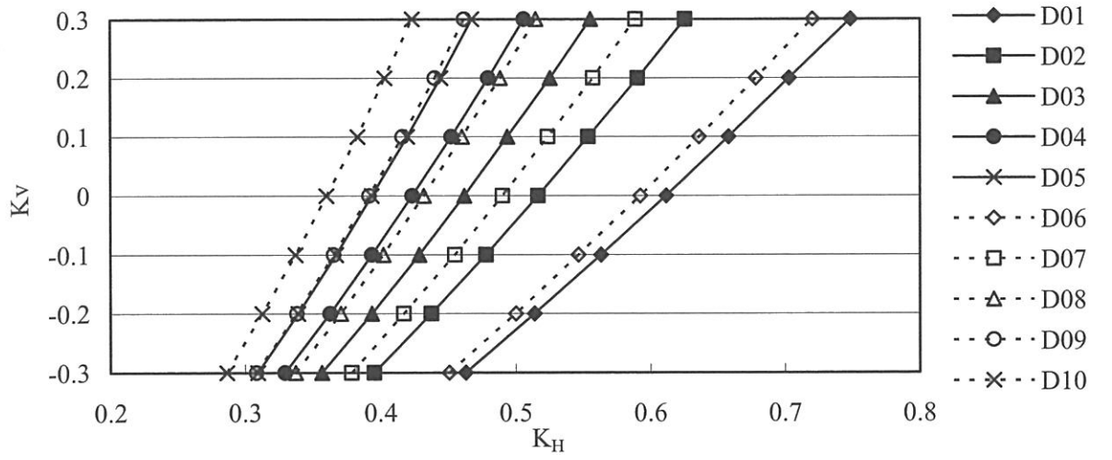

Figure 5. Relation of yield acceleration Kv and K_H.

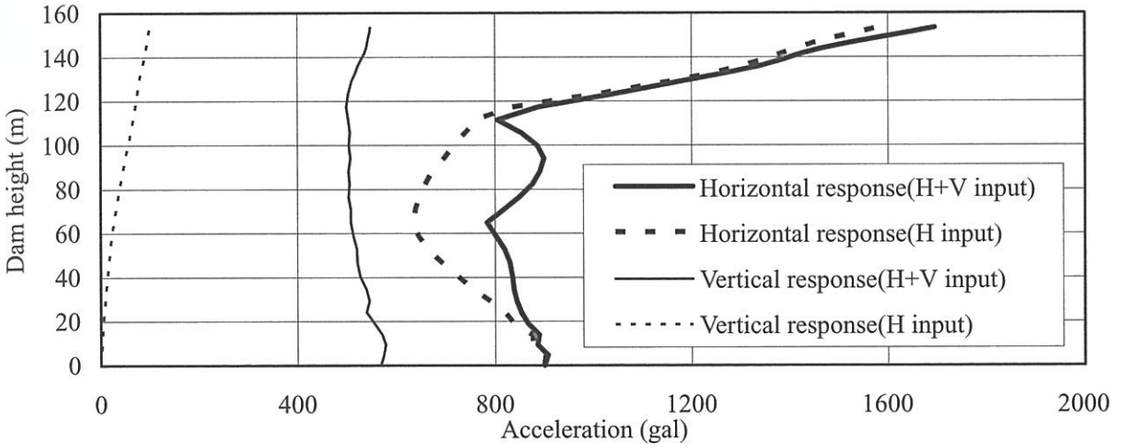

Figure 6. Maximum acceleration with and without vertical motion input.

Table 2. Acceleration records used for the analysis.

Earthquake	Dam	Year	Magnitude	Duration (s)	PGA (gal) Up-down stream	Cross canyon	Vertical	Case no
Kobe	Hitokura	1995	M7.3	10.48	182	168	63	CASE01
Kobe	Gongen			24.00	104	90	66	CASE02
Kobe	Mino			59.21	135	128	80	CASE03
Tottori	Gasho	2000	M7.3	60.00	494	569	485	CASE04
Tokachi	Urakawa	2003	M7.9	173.68	103	100	66	CASE05
Tokachi	Takami			70.41	56	–	41	CASE06
Chuetsu	Sabaishi	2004	M6.8	15.12	230	231	213	CASE07
Noto	Hakkagawa	2007	M6.7	100.00	167	203	167	CASE08
Chuetsu	Kakizaki	2007	M6.8	120.00	170	143	76	CASE09
Iwate-Miyagi	Kurikoma	2008	M7.2	100.00	461	276	402	CASE10

more effects on the vertical response than on the horizontal one. Therefore, when the vertical response is taken into Newmark sliding block analysis, vertical motion input is a must.

5 RESPONSE AND SETTLEMENT TO SINUSOIDAL INPUT MOTION

To study the effect of the phase difference of horizontal and vertical input motions, the sinusoidal motion was used for the analytical model of Figure 3. The period of sinusoidal motion is 0.5 s (f = 2 Hz) for both of horizontal and vertical input and maximum acceleration of horizontal and vertical is 0.75 g and 0.5 g, respectively. The phase was staggered by $\pi/4$ for horizontal and vertical inputs.

Horizontal input: $Ah\,(t) = 0.75g \sin(2\pi ft)$
Vertical input: $Av\,(t) = \sin(2\pi ft + n\pi/4)$
where, n = 0, 1, 2, 3, 4, 5, 6, 7 and $A_v(t) = 0$

The duration of the motion is 5.12 s and the envelope coefficient was multiplied by the sinusoidal input. Figure 7 shows the vertical input motions in the cases, n = 0 (phase difference 0) and n = 4 (phase difference π).

Figure 8 shows the settlements of sliding block D03. Here, the settlement is defined as the vertical displacement at the upper tip of the sliding block as a result of its rotational

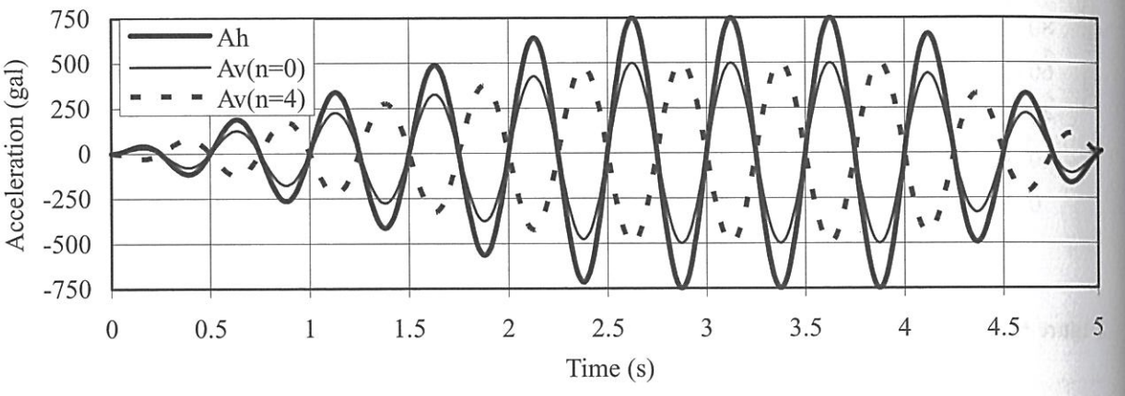

Figure 7. Sinusoidal input motion with phase difference.

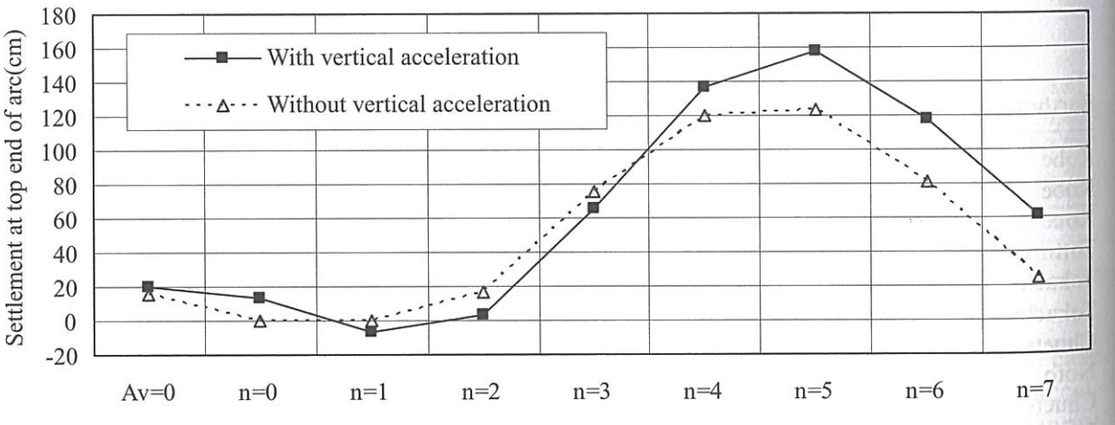

Figure 8. Settlement of sliding block D03 to different phase vertical motions.

movement. This figure indicates that settlement varies with the vertical motions of different phases regardless of whether or not the vertical response acceleration is taken into account. This is due to the vertical motion input of different phase affecting the horizontal response acceleration. In cases n = 4 to 7 (phase difference π to $7\pi/4$), the settlement was greater when the vertical response acceleration is considered. The case n = 5 gives the maximum settlement of 160 cm when horizontal and vertical acceleration are taken into account and 120 cm without vertical acceleration.

6 RESPONSE AND SETTLEMENT TO EARTHQUAKE INPUT MOTIONS

The acceleration time histories recorded at foundations of 10 dams as shown in Table 2 are used to perform dynamic analyses. Here the Tokachi Earthquake is an earthquake with hypocenter on the subduction plate boundary. The other earthquakes occurred in the shallow crust.

The acceleration time histories are normalized to a maximum acceleration of 0.75 g. Their frequency characteristics are distributed in a wide range. Figure 9 shows the time histories of the resisting moment and driving moment for sliding block D09 in CASE06, which gives relatively large settlement. The top figure shows the moment with horizontal and vertical response acceleration while the bottom gives the moment with horizontal response acceleration only. Comparing the top and bottom, the vertical response acceleration seems to have less effect on the driving moment and more effect on the resisting moment. This diagram also shows that the duration the driving moment exceeds the resisting moment becomes longer for taking the vertical response into consideration into account, resulting in larger settlement.

The correlation of settlements with and without vertical accelerations is depicted in Figure 10. The figure shows that the ratio of the settlement with and without vertical acceleration varies from 0.6 to 1.4 excluding cases of very small settlements and uppermost slip surfaces of D01 and D06.

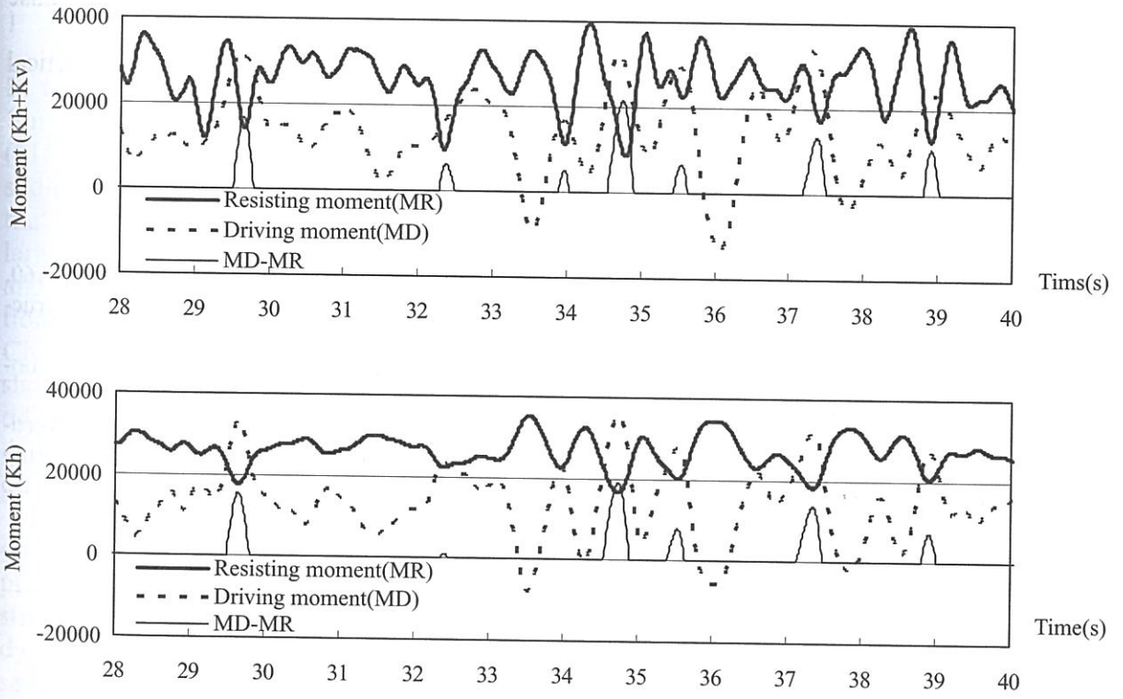

Figure 9. Time histories of resisting and driving moments (CASE06 in Table 2).

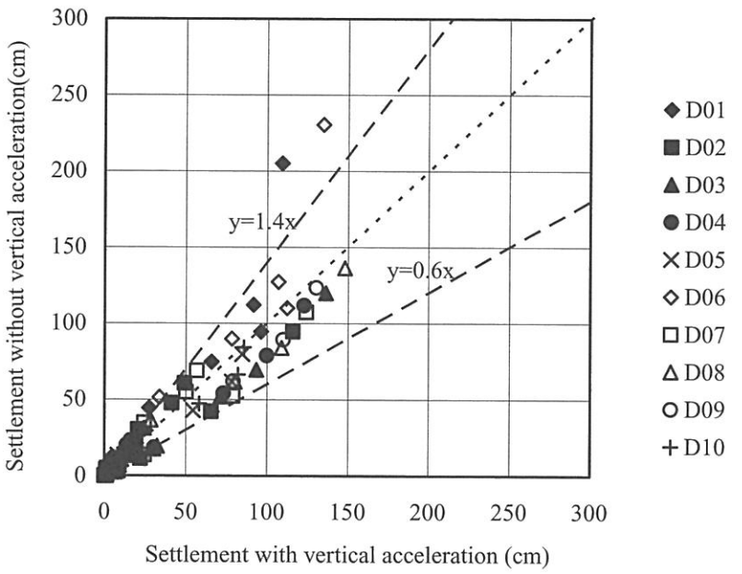

Figure 10. Settlements with and without vertical acceleration for slip surfaces D01 to D10 (Fig. 3).

7 CONCLUSIONS

The following conclusions can be drawn from this study:

1. When the curved failure envelope is used for the strength evaluation of the slip surface, the deeper the sliding surface is, the smaller the yield acceleration is. In this case, the larger and deeper the arc is, the smaller the effect of the vertical seismic coefficient on the sliding safety factor is.
2. In the case of the sinusoidal acceleration input with the period of 0.5 sec and the duration of 5.12 sec, the maximum settlements with the vertical acceleration and without are 160 cm and 120 cm, respectively. This effect of vertical acceleration varies with its phase of input vertical motions.
3. In the case of earthquake input motions the ratio of settlement with and without vertical acceleration is mostly in a range of approximately 0.6 to 1.4.

REFERENCES

Newmark, N.M. 1965. Effects of earthquakes on dams and embankments. *Geotechnique, 15(2)*: 139–160.

Tateyama, M. Tatsuoka F. Koseki J. & Horii K. 1998. Studies on Seismic Design Method of Soil Structures. Railway Technical Research Institute, Vo. 12, No. 4: 7–12.

Yan, L. 1991. Seismic deformation analysis of earth dams: A simplified method, Soil Mechanics Laboratory Report, No. SML 91–01: California Institute of Technology.

Yan, L. Matasovic N. & Kavazanjian E. 1996. Seismic response of a block on an inclined plane to vertical and horizontal excitation acting simultaneously. Proceedings of 11th Conference on Engineering mechanics, ASCE, Fort Lauderdale, FL: 1111–1113.